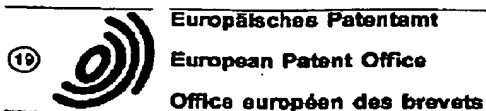


BEST AVAILABLE COPY



(11) Publication number: **0 509 843 A2**

(12)

EUROPEAN PATENT APPLICATION

(21) Application number: **92303498.7**

(51) Int. Cl.⁵: **G01S 13/42, G01S 13/22,
G01S 13/58, G01S 13/87**

(22) Date of filing: **16.04.92**

(30) Priority: **16.04.91 US 685781**

(43) Date of publication of application:
21.10.92 Bulletin 92/43

(84) Designated Contracting States:
DE FR GB IT

(71) Applicant: **GENERAL ELECTRIC COMPANY**
1 River Road
Schenectady, NY 12345 (US)

(72) Inventor: **Freedman, Jerome Edwin**
742 Mill Street
Moorestown, New Jersey 08057 (US)
Inventor: **Perry, Michael Stockum**
300 Millside Lane
Haddonfield, New Jersey 08033 (US)
Inventor: **Gallagher, John James**
18 Pembroke Drive
Turnersville, New Jersey 08012 (US)

(74) Representative: **Lupton, Frederick**
LONDON PATENT OPERATION, G.E.
TECHNICAL SERVICES Co. INC., Essex
House, 12/13 Essex Street
London WC2R 3AA (GB)

(64) Radar system with active array antenna, elevation-responsive PRF control, and beam multiplex control.

(57) A multipurpose system provides radar surveillance for air traffic control purposes. The system includes four separate active phased-array antennas, each with $\pm 45^\circ$ coverage in azimuth, from 0° to 60° in elevation. Each antenna element of each phased-array antenna is coupled by a low-loss path to the solid-state amplifier associated with a transmit-receive (TR) module. Each antenna produces a sequence of pencil beams, which requires less transmitted power from the TR modules than a fan beam, but requires more time because the pencil beam must be sequenced to cover the same volume as the fan beam. In order to scan the volume in a short time, the PRF is responsive to the elevation angle of the beam, so higher elevation angles use a higher PRF. Low elevation angle beams receive long transmitter pulses for high power, and pulse compression is used to restore range resolution, but the long pulse results in a large minimum range within which targets cannot be detected. A second scan is provided at low elevation angles with a short transmitter pulse to fill in the short-range coverage. Beams at higher elevation angles transmit pulse widths which are shorter than beams at low elevation angles, so that the minimum range requirement is met without a second scan, which also reduces the time required for volumetric scan. The number of pulses which are integrated to produce a return increases off-axis, to restore system margin lost due to off-axis power gain reduction. The volumetric scan rate is increased by a dynamic scan regimen by which subsets of beams are pulsed with a high transmitter PRF but with a low effective beam PRF to reduce range ambiguity and preserve Doppler resolution without the usual increase of scan time. For best range resolution, Doppler processing is used, with range sidelobe pulse suppression applied separately to each Doppler frequency bin.

EP 0 509 843 A2

Jouve, 18, rue Saint-Denis, 75001 PARIS

EP 0 509 843 A2

This invention relates to radar systems, and especially to radar systems intended for operation with targets which are known to be below a predetermined altitude.

The volume of air transportation is placing increasing demands on air traffic control systems. Air traffic control systems may utilize surveillance radar systems for detection of aircraft approaching and within a controlled region, beacon systems for activating transponders on aircraft equipped therewith, communications between air traffic controllers and aircraft, wind shear detectors, weather radar, terminal approach systems, terminal approach systems for use with parallel runways, wake vortex monitoring, and possibly other functions. The various equipments required at each airport are individually expensive, their independent siting requires extensive installation and large land area, and also requires extensive communications lines and facilities for interconnection of the equipments with a control center. The independent sites must each be provided with security and maintenance, which increases costs. Present air traffic control primary surveillance radars such as the ASR-9 are mechanically scanned fan-beam systems.

Mechanically scanned reflector antennas for surveillance use generally use a "cosecant squared" fan-beam radiation pattern to provide coverage in elevation while scanning in azimuth. mechanically scanned systems cannot advantageously be adapted for common use for tracking and either final-approach control or atmospheric-disturbance monitoring, because the reflector antenna has substantial inertia, and cannot be moved quickly from one position to another. In radar, any condition generating a reflection, such as an aircraft or a localized weather phenomenon, is termed a "target". For aircraft final approach control, the delay from one rotation of the reflector antenna to the next is so long that proper aircraft control may not be possible under all circumstances, especially with high-speed targets such as aircraft, and atmospheric disturbance targets may change or move significantly during a rotation. Long pulse repetition intervals (PRI) are required to provide unambiguous coverage over long distances using pulse Doppler waveforms. The long PRI requires the rotating-reflector antenna to dwell for a relatively long time at each incremental azimuth position, so the antenna rotational speed cannot be increased without reducing its maximum unambiguous range. For an instrumented range (maximum range for which the equipment is designed and optimized) of 60 nautical miles (nm), the ASR-9 completes a 360° scan in about 5 seconds. One nautical mile equals 1852 meters or 1.1508 statute miles.

The long-range requirement also requires the use of relatively high transmitted power to reliably detect small targets. High transmitted power implies a relatively higher peak transmitter power or a longer duration transmitter pulse (also known as a "wider" pulse). Assuming a maximum available peak power, longer range implies a longer duration transmitted pulse. A longer duration pulse tends to reduce range resolution, which is the ability to distinguish among targets which are at similar ranges. Pulse compression techniques can be used to improve range resolution in spite of the longer pulse duration, thus eliminating the need for high peak power short pulses, but the minimum range at which a target can be detected increases with the transmitted pulse length. Thus, if the transmitter pulse duration is 100 microseconds (μs), the minimum distance at which a target may be detected is about 8 nautical miles (nm). Clearly, a surveillance radar using pulses of such a duration cannot be used to detect aircraft which are landing or taking off from an airport. An additional problem associated with pulse compression is the appearance of range sidelobes (as distinguished from antenna sidelobes) in addition to the main range lobe. The time position, or range, of the main lobe is the position that is tested for the presence of a target and for estimating the parameters of that target (reflected energy or power, closing speed, fluctuations in echo power and closing speed, etc.). The presence of range sidelobes on the compressed pulse results in interfering echoes which originate at ranges other than the range of the main lobe. This interference, known as "flooding" can cause erroneous estimates of the echo characteristics in the range cell (i.e., range increment) covered by the main lobe. Prior art techniques for suppressing range sidelobes include the "zero-Doppler" technique, in which the range sidelobe suppression scheme is based in part upon the assumption that the interfering echoes, as well as the desired echo, have a closing velocity that has no significant Doppler phase change or shift over the duration of the uncompressed pulse. The Doppler phase shift ϕ_{DV} across the uncompressed pulse is 2π times the product of the Doppler frequency shift and the uncompressed pulse duration (i.e. $\phi_{DV} = 2\pi f_d T_0$ radians). When this Doppler phase shift is actually zero or very small, moderate sidelobe suppression is achievable with the zero Doppler design. However, the zero Doppler design is very sensitive to small Doppler frequency shifts, making deep sidelobe suppression impossible for applications in which very deep sidelobe suppression is desired, as in weather mapping, clear air turbulence detection, and microburst detection.

Electronically scanned array antennas are inertialess, and may be capable of rapid scanning. The rapid scanning ability gives rise to the possibility that various air traffic control and atmospheric monitoring uses could be multiplexed with the surveillance. An array antenna using a centralized power transmitter and a "corporate" feed has lossy transmission-line components, including power splitters, between the transmitter and the element of the array antenna. Such losses may make it difficult to achieve the desired power gain with antennas of reasonable size, low-power phase shifters, and moderate-power transmitters.

EP 0 509 843 A2

An active phased-array radar may provide improved reliability over a single-transmitter radar by virtue of its many transmitter modules. Also, it may provide high power gain by virtue of its many transmitter modules, and because power losses occur at low power levels before final amplification, which results in low power losses between the transmitters and their antennas. The active antenna architecture also provides reduced system noise during reception because the majority of the receiver losses follow low-noise amplification. Because of the inertialess scanning, it provides the possibility of integration of functions other than surveillance, thereby providing an overall cost reduction.

Summary Of The Invention

A radar apparatus for detection of targets includes a controllable signal generator with a pulse recurrence frequency (PRF) control input port, for generating pulses of radio frequency signals at a recurrence frequency which is controlled by PRF control signals applied to the control input port. According to an aspect of the invention, a controllable active array antenna is coupled to the signal generator. The antenna has a thinned aperture. The antenna includes a control input port, and is adapted for responding to the radio frequency (RF) signals by transmitting at least one pencil beam in a direction established by control signals applied to the control input port of the antenna. An elevation determining arrangement is coupled to the control input port of the antenna for generating elevation angle control signals for directing the beam of the antenna in a predetermined direction. According to an aspect of the invention, the signal generator is coupled to the elevation determining arrangement for control of the recurrence frequency in response to the elevation control signals. In a particular embodiment of the invention, the PRF control signals are generated at a relatively high rate (as high as 15 or 16 KHz) when the elevation control signals direct the beam to a relatively high elevation angle (near 60°), and the PRF signals are generated at a relatively low rate (near 1 KHz) when the elevation control signals direct the beam at a relatively low elevation angle (near 0°). According to another aspect of the invention, the volumetric scan is speeded by a beam multiplex mode of operation, in which the pencil beam alternates between spaced-apart positions during sequential transmit/receive intervals, so that a portion of the interpulse time otherwise used only for range ambiguity reduction is used to derive additional useful information. In a particular embodiment of the invention, the pencil beam alternates in azimuth angle about positions spaced apart in azimuth by at least 12°. According to another aspect of the invention, the volumetric scan is speeded by using relatively short transmitter pulses at high elevation angles and relatively long pulses at low elevation angles, whereupon only the low elevation angles need to be scanned again with short pulses to fill in the short-range coverage. In a particular embodiment of the invention, pulses of 100 μ S duration are transmitted at elevation angles below about 10°, and pulses of 1 μ S duration are transmitted at elevation angles above about 15°. According to another aspect of the invention, the loss of gain or signal-to-noise margin occasioned by scanning the pencil beam off-axis is compensated by relatively increasing the number of pulses transmitted on each beam compared with the relatively smaller number which is transmitted on axis, which increases the total power transmitted in directions in which antenna gain is lower. According to another embodiment of the invention, Doppler processing is used to separate returns into frequency bins representative of radial speed, and interference from scatterers at other ranges is reduced by range sidelobe suppression applied to the signals in each frequency bin. Other ancillary aspects of the invention are described below.

Description Of The Drawing

FIGURE 1 is a perspective or isometric view of a shelter or building adapted for supporting phased-array antennas;
FIGURE 2a is a simplified functional block diagram illustrating a method for establishing energy distribution between a feed point and one of the arrays of FIGURE 1, and also illustrating some details of the array, and FIGURE 2b is a simplified functional block diagram of a transmit-receive (TR) module which may be used with the arrangement of FIGURE 2a; FIGURES 2a and 2b are together referred to as FIGURE 2;
FIGURE 3a is a simplified block diagram of a radar system according to the invention, FIGURE 3b is a simplified schematic diagram of a portion of FIGURE 3a for implementing PRI and beam multiplex control, FIGURE 3c is a simplified block diagram of a portion of FIGURE 3a for implementing off axis beam integration control, and FIGURE 3d is a simplified flow chart illustrating the operation of the arrangement of FIGURE 3c. FIGURES 3a, 3b, 3c and 3d are referred to together as FIGURE 3;
FIGURE 4 illustrates the thinning of the aperture of the array antenna of FIGURE 2;
FIGURE 5a illustrates the elevation radiation pattern of a fully populated, uniformly illuminated aperture as a reference, and FIGURE 5b illustrates the elevation radiation pattern of the thinned aperture of FIGURE 4, with uniform power applied to the elements of the array;

EP 0 509 843 A2

FIGURES 6a and 6c together illustrate all the beams generated in one octant by the thinned array of FIGURE 4, and FIGURE 6b is a detail thereof; FIGURES 6a, 6b and 6c are jointly referred to as FIGURE 6; FIGURE 7 illustrates in superposed form the elevation radiation patterns of several pencil beams sequentially produced by the antenna of FIGURE 4, showing how complete coverage is obtained to a specific altitude and range;

FIGURES 8a and 8b are elevation angle representations of the beams of FIGURES 6a and 6c, showing slant range coverage;

FIGURE 9 illustrates a time line;

FIGURE 10 tabulates summarized parameters of an embodiment of the radar as a function of angle; and

FIGURES 11a-11p tabulate details of the number of pulses per beam as a function of azimuth angle for each elevation angle of the beam structure of FIGURE 6, and also tabulates elapsed time per beam; and FIGURES 12a-12g are partial flow charts, together representing the logic for control of a radar according to the invention;

FIGURE 13 is a simplified block diagram illustrating a prior-art processor for pulse compression, range side-lobe reduction and Doppler filtering;

FIGURE 14a is a simplified block diagram of a corresponding processor according to an embodiment of the invention, and FIGURE 14b is a simplified block diagram of a portion of the arrangement of FIGURE 14a;

FIGURE 15a is a simplified block diagram of another processor for performing the same processing as in FIGURE 14a, FIGURE 15b is a simplified block diagram of a portion of the arrangement of FIGURE 15a, FIGURE 15c is an alternative to FIGURE 15b, and FIGURE 15d is another embodiment of the invention; and

FIGURE 16 is an amplitude-frequency representation of the effect of processing in accordance with FIGURES 14 and 15.

Description Of The Invention

FIGURE 1 is a perspective or isometric view of a building or structure. Structure 10 is in the form of a truncated quadrilateral pyramid including faces or sides 12 and 14. Structure 10 sits atop a base or foundation 16. Each face 12, 14 of structure 10 bears a planar array antenna 18. Array antenna 18a is associated with face 12, array antenna 18b is associated with face 14, and two other array antennas are associated with the two hidden faces of structure 10. Those skilled in the art of array antennas know that array antennas such as 18 may be two-dimensional arrays of hundreds or thousands of antenna elements, which may be used with either a space feed or a constrained "corporate" feed, and with phase-shifters for scanning along one or two axes. One conventional axis is azimuth angle ϕ , measured in the x-y plane relative to the $\phi=0^\circ$ axis, illustrated in FIGURE 1. Another angle which is commonly used is the zenith angle, measured from the zenith or z axis. An alternative to the zenith angle is the elevation angle θ , measured from the horizontal x-y plane.

A portion of antenna 18b is illustrated in simplified functional form in FIGURE 2a. Antenna 18b includes a face portion designated generally as 19 together with a feed portion designated generally as 30. In FIGURE 2a, face portion 19 is illustrated in cross-section, and its outer, visible "front" face is illustrated as a dash-line 20. A plurality of antenna elements 22a, 22b, 22c...22n are illustrated as being associated with front face 20. Line 20 may be considered to be the edge of a plane which is the locus of the phase centers of antenna element 22. A dash-line 24, which is orthogonal to front face 20, represents the broadside direction relative to the array. Reference azimuth $\phi = 0^\circ$ is the projection of broadside line 24 onto a horizontal plane. Front face 20 of array antenna 18b is tilted relative to the horizontal so that broadside direction line 24 makes an elevation tilt angle θ_T with the horizontal. In a particular embodiment of the invention, θ_T is selected to be 15° . Thus, broadside direction 24 of the antenna array is tilted at an elevation angle of 15° above horizontal azimuth reference line $\phi = 0^\circ$.

Each elemental antenna 22a, 22b...22n of FIGURE 2a is associated with a bidirectional transmit-receive (TR) processor or module illustrated as a block 26. Thus, elemental antenna 22a is associated with a TR module 26a, elemental antenna 22b is associated with TR module 26b, and elemental antenna 22n is associated with a TR module 26n. As described below, each TR module may include a power amplifier, one or more phase shifters, a low noise amplifier, and multiplexing or diplexing arrangements. A bus conductor line 42 carries operating power and control signals for the operating mode, for the phase shifters, and the like, to TR modules 26.

In accordance with an aspect of the invention, the signal source driving each of the TR modules in a transmit mode is a further elemental antenna 28, and the load on each of the TR modules in the receive mode is the same elemental antenna 28. As illustrated in FIGURE 2a, this further set of elemental antennas, termed inner

EP 0 509 843 A2

antenna elements, is illustrated as 28a-28n. Thus, inner antenna element 28a is coupled to a port of TR module 26a, inner antenna element 28b is coupled to TR module 26b, and inner antenna element 28n is coupled to TR module 26n. A plane 34 represents the locus of the phase centers of inner antenna elements 28.

5 A central monopulse space feed arrangement is illustrated generally as 30 in FIGURE 2a, and includes a monopulse horn antenna 32 located near the projection of boresight 24, and spaced away from plane 34. Horn 32 is fed with radio-frequency (RF) signal from a circulator 36, which in turn receives the signal from a transmitter (not illustrated in FIGURE 2a) by way of a transmission line 38. The term radio frequency for this purpose includes microwave and millimeter-wave frequencies. Horn 36 generates sum and difference monopulse signals from the signals which it receives from antennas 28, and the sum and difference signals are coupled by separate
10 sum and difference channels (not separately illustrated) from horn 32 to a receiver (not illustrated in FIGURE 2a) by way of circulator 36 and a further transmission line 40.

FIGURE 2b is a simplified block diagram of a TR module which may be used in the system of FIGURE 2a. For definiteness, FIGURE 2b illustrates representative module 26b of FIGURE 2a. In FIGURE 2b, signals entering inner antenna 28 are routed by a circulator 208 to a controllable phase shifter 210, which controls the
15 phase shift in accordance with commands received over a portion of data path 42. The commands select the phase shift to define the characteristics of the transmitted antenna beam. Phase shifter 210 may have an attenuation characteristic which changes in response to the commanded phase shift. A variable attenuator illustrated as 212 may be cascaded with phase shifter 210 and controlled in a manner which compensates for the attenuation of phase shifter 210. The constant-amplitude, phase shifted signals are coupled from the output of
20 attenuator 212 to the input of a power amplifier (PA) 214. PA 214 amplifies the signal to produce a signal to be transmitted, which is coupled by way of a circulator 216 to antenna 22b for radiation into space. Returning signals reflected from targets are received by antenna 22b, and are coupled to circulator 216. Circulator 216 circulates the received signal to a low noise amplifier (LNA) 218, which amplifies the signal to maintain the signal-to-noise (S/N) ratio during further processing. The amplified received signal is coupled from LNA 218 to a
25 phase shifter 220, which is controlled by signals received over a portion of data path 220 in a manner selected to define the receive antenna beam. The phase-shifted, received signals are circulated by circulator 208 to inner antenna 28b for radiation back to antenna 32 of FIGURE 2a. Those skilled in the art know of many modifications which may be made to the general structure of FIGURE 2a. In particular, the attenuation or loss of circulators 208 and 216 may be reduced by substituting controlled switches therefor, and the switches may be controlled
30 by way of bus 42 during prescribed transmission and reception intervals.

Those skilled in the art know that antennas are passive reciprocal devices which operate in the same manner in both transmitting and receiving modes. Ordinarily, explanations of antenna operation are couched in terms of only transmission or reception, the other mode of operation being understood therefrom. Elemental
35 antennas 22 and 28, and horn antenna 32 of FIGURE 2 operate in both transmission and reception modes depending upon the mode of operation of the radar system. Thus, the description herein, while referring to transmission and reception, as appropriate, should not be interpreted to exclude the other operation. One central space feed 30 is associated with each array antenna 18. An antenna array having a transmit amplifier associated with each antenna element is known as an "active" array. Active array antenna 18a has a central feed 30 independent of the corresponding feed for array antenna 18b.

40 In operation, horn 32 of FIGURE 2 is fed with low-level transmitter pulses, which are radiated as an electromagnetic field toward antennas 28. Antennas 28 receive the pulses, and couple the resulting low-level signal pulses to TR modules 26. Each TR module phase-shifts its signal by an amount determined by appropriate beam direction control signals applied over bus 42, amplifies the resulting phase-shifted signal, and applies the amplified signal to an antenna element 22 by a path which includes no discrete attenuator (although all
45 paths include inherent attenuation). While each solid-state TR module 26 can produce only a relatively low power, the cumulative result of this process performed over the entire aperture of antenna 18b is the generation of a pulse of high-power radiation transmitted in the desired direction. After each pulse is transmitted, as described below, the system reverts to a receive mode, by which signal received at each elemental antenna 22 is coupled to its TR module to be amplified by its low-noise amplifier 218, and the amplified received signal is
50 passed through the controlled phase shifter 220, to be radiated by the corresponding elemental inner antenna 28. The cumulative effect of radiation by all such inner antennas is to radiate a beam of amplified received signal back toward monopulse horn 32. Horn 32, in turn, separates the received signal into sum and difference signals, and couples the cumulated received sum and difference signals through circulator 36 to the system receivers as described below. During reception, the beam may be pointed in the direction of the preceding transmission,
55 or in another direction, also as described below.

FIGURE 3a is a simplified block diagram of a system in accordance with the invention. Elements of FIGURE 3a corresponding to those of FIGURES 1 and 2 are designated by the same reference numerals. Active antenna 18b is at the right of FIGURE 3a. The beam direction of antenna 18b is controlled by beamsteering logic (BSL)

EP 0 509 843 A2

illustrated as a block 48, which receives timing and control signals over a data bus 42 from a timing and control signal unit (TCU) 58. It should be emphasized that BSL 48 may be an external unit which feeds command data in common to all the TR modules, or each TR module may contain its own portion of the BSL for reducing the amount of data which must be routed to each TR module. Central radio-frequency feed 30 of antenna 18b is coupled by transmission lines 38 and 40 to a transmit-receive (TR) multiplex (MPX) arrangement illustrated as a block 50. In a receive mode, multiplexer 50 receives low-amplitude or low-level signals from RF feed 30, as described above, and couples the RF signals from central RF feed 30 to a receiver Analog Signal Processor (RCVR/ASP) illustrated as a block 52. A radio frequency waveform generator (WFG) illustrated as a block 54 provides low-level reference local oscillator (LO) signals to receiver 52 in a receive mode, and also provides low-level transmitter waveforms by way of a transmission line 56 to multiplexer 50. multiplexer 50 also receives timing and control signals by way of a bus 59 from a timing and control unit (TCU) 58 for controlling its operation to couple low level transmitter waveforms to RF feed 30 in a transmit mode, and for thereafter providing a path by which received sum-and-difference signals may be coupled to receiver 52.

Received signals, in sum and difference channels, if appropriate, are downconverted and low-noise amplified in block 52 of FIGURE 3a, and the resulting downconverted or baseband signals are coupled by way of transmission lines illustrated as 60 to analog-to-digital converters (ADC) illustrated as part of a block 62. Block 62 also includes a buffer for storing digitized received signals as described below, all under the control of timing and control signals received from TCU 58 by way of a data path 64. The analog-to-digital conversion is performed at a "range" clock rate, which defines the smallest discernible range increment. Digitized sum in-phase and quadrature signals, and digitized difference in-phase and quadrature signals, together representing the target returns to antenna 18b, are coupled from ADC and buffer 62 of FIGURE 3 over a data path 66 to a Digital Signal Processor (DSP) illustrated as a block 68.

DSP block 68 of FIGURE 3a performs the functions of (a) pulse-to-pulse Doppler filtering by means of a Fast Fourier Transform (FFT) algorithm, with data weighting to control signal leakage from neighboring Doppler shifts (frequency leakage); (b) digital pulse compression; (c) range sidelobe suppression; and (d) further signal processing including CFAR (constant false alarm rate) processing, thresholding for target detection, spectral processing for weather mapping, etc. Items (a), (b), and (d) are performed in ways well understood in the art, and form no part of the invention. The range sidelobe suppression (c) is advantageously Doppler tolerant as described below in conjunction with FIGURES 13-16. The results of the processing done in block 68 may include (a) target detection reports (aircraft); (b) radar track detection reports; (c) weather components for each resolvable volume of space, including (c1) echo intensity; (c2) echo closing speed, and (c3) spectral spread of the echo, and these components of information may be included in Digitized Radar Detection Reports (DRDR). The DRDR reports may also include data relating to the angular coordinates of the antenna beam in which the detection occurred, the range of the detection, the monopulse sum and difference values extracted from the digitized received signals, and the PRF of the dwell in which the detection occurred. The target ID may also be included if the detection occurs in a tracking beam. The DRDR reports are applied over a data path 70 to Detection Processor (DP) block 72.

In generating the DRDR reports, DSP block 68 of FIGURE 3a performs pulse Doppler and moving target Indicator (MTI) or moving target detector (MTD) filter processing. A person skilled in the art of pulse compression will know that the radar pulse must be coded in some manner that allows DSP block 68 to correlate received signals with the known transmitted pulse code. The correlation process simultaneously improves the signal to noise ratio and the range resolution of target echoes. A person skilled in the art knows that a variety of satisfactory pulse coding techniques are available in the prior art. Such techniques include the well known Barker Codes, pseudorandom noise codes, and linear FM coding techniques. DSP block 68 therefore also performs digital pulse compression on the received signals.

The processed amplitude output of the sum channel is also compared to a detection threshold level in DSP block 68 of FIGURE 3a, and if the amplitude exceeds the threshold a detection is declared, and the above-mentioned range, sum and difference values and other data are formatted into the Digitized Radar Detection Reports and communicated to DP block 72 via data path 70. A person skilled in the art of radar detection will know how to set the threshold level according to the radar characteristics and the desired probability of detection (Pd) and probability of false alarm (PFA), and he will know how to design the threshold detector to use a smoothed estimate of interference and outputs from the moving target detector (MTD) to yield a detection process that has the characteristic of a Constant False Alarm Rate (CFAR) detector. DSP block 68 can be implemented in a variety of embodiments, including 1) specially designed hardware which performs only the specific processes required for the DSP; 2) a high speed general purpose computer which is programmed to perform the specific processes required for the DSP; 3) a high speed general purpose array processor which is programmed to perform the specific processes required for the DSP; and 4) combinations of the above.

Detection Processor block 72 receives the DRDR reports, including track reports (defined below), from DSP

EP 0 509 843 A2

block 68 by way of data path 70 and processes the digitized sum and difference values to estimate monopulse corrections, and adds the corrections to the beam angular coordinates to calculate the angular position of the detected target. Detection Processor block 72 also calculates the range and range rate of the detected target. Detection processor 72 appends the processed range, angles and range rate to the digitized detection report and sends the resulting DRDR reports and track reports to Radar Control Computer (RCC) block 78 by way of data path 76, and to other external users over a data path 74. RCC block 78 uses the detection and track reports to identify new targets, to identify maneuvering targets, to identify dedicated tracks, and to update track files, and also uses the results to construct new sets of control parameters according to the Radar Scheduling Control Program (RSCP) illustrated as block 80 in FIGURE 3 and further described below in conjunction with FIGURES 12a-g. The Radar Scheduling Control program actually resides in Radar Control Computer block 78.

FIGURE 4 illustrates the thinning of the aperture of the array of antenna 18b. Thinning of the aperture is an aspect of the invention which may advantageously be used in conjunction with other aspects of the invention. As illustrated in FIGURE 4, the rectangular aperture includes 55 columns in which an antenna element may appear, and 59 rows, for a total of 3245 locations or "slots". In a fully populated array, the row spacing is such that elements are required in every other row to implement a triangular element lattice. Column 1 of a fully populated aperture contains elements in odd numbered slots 1 to 59 for a total of 30 elements, column 2 contains elements in even numbered slots 2 to 58 for a total of 29 elements. Therefore, every other slot is filled, and the fully filled or populated aperture (a non-thinned aperture) contains 1623 elements located in 3245 slots. The existence of an antenna element (and its corresponding transmit-receive module and inner antenna) in a slot (a member of the population) of the thinned array is represented in FIGURE 4 as a numeral "1" located at the intersection of the corresponding row and column. The absence of a numeral "1" indicates that the thinned array includes no antenna element at that location. Column 57 of FIGURE 4 lists a numeral in each row, which represents the number of antenna elements of the thinned distribution in the row, and column 58 shows the number 829, which represents the total number of elements. Row 62 similarly includes numerals representing the total number of elements in each column, and the total of those numbers appears in row 65 as a check.

The thinning of the array is in accordance with probability based upon a Taylor distribution. This type of thinning is described in the July, 1984 issue of IEEE Transactions on Antenna and Propagation, at page 408 in an article by Skolnik et al. Naturally, other thinning distributions may provide satisfactory performance for some purposes. The thinning reduces the antenna element density near the edges of the aperture compared with the density near the center of the aperture. Those skilled in the antenna arts know that an element distribution of this sort generates an antenna pattern with relatively low sidelobes compared with a uniform distribution of the elements. Thus, thinning illustrated in FIGURE 4 avoids the need for modulating the power output of each TR module 26 of FIGURE 2. That is, the power amplifier 214 of each TR module 26 can operate at the same output power, and the effective amplitude distribution across the aperture of the antenna array is such as to yield desirable sidelobe levels and beam shapes. If each radio-frequency amplifier (214 of FIGURE 2b) produces the same amount of power to be radiated, the thinning eliminates the need for an attenuator following each power amplifier 216 for controlling the power to taper a fully populated aperture. Not only does this type of thinning reduce the need for a power output controlling attenuator associated with each TR module, but all TR module transmitter amplifiers can be identical units which operate at the same maximum output power level and therefore at maximum efficiency and therefore yield the highest possible transmitted power gain product. This is particularly important when solid-state radio-frequency (microwave or millimeter-wave) amplifiers are used, which at the present state of the art tend to be limited in available output power by comparison with vacuum tubes. The thinning is also advantageous from a cost viewpoint because control buses for the attenuators need not be provided, the number of TR modules in the populated antenna aperture is less than in a fully populated aperture, and each of the modules may be fabricated without an attenuator. It should be noted that while, as described above, it is advantageous to avoid use of an attenuator between the final radio frequency amplifier and the associated antenna element, it is not possible to avoid attenuation which is inherent in the various components and elements in the interconnection. If these interconnections include variable elements such as variable phase shifter 210 of FIGURE 2b, the unavoidable attenuation or loss may even be variable. Consequently, if the path between the inner antenna 28 and the RF power amplifier includes a variable phase shifter such as 210 controlled for directing the beam, an associated attenuator such as 212 may be required in order to equalize the attenuations of the various phase shifters and to maintain constant effective PA output power.

FIGURE 5a illustrates a computer simulation of an elevation radiation pattern of a fully filled or fully populated aperture of 1623 uniformly distributed elements. The pattern of FIGURE 5a is made at $\phi = 0^\circ$, the vertical plane in which the broadside axis (24 of FIGURES 1 and 2) lies. As illustrated in FIGURE 5a, the first sidelobes are about 14 dB down. FIGURE 5b illustrates a distribution according to FIGURE 4, having 829 elements, all of equal amplitude. As illustrated in FIGURE 5b, the main beam 510 is narrow and symmetric, and the sidelobe level is more than 20 dB down. The simulated element errors for FIGURE 5b are 0.1 Volts/Volt maximum rms

EP 0 509 843 A2

amplitude error (10% error) and 18.71 degrees maximum rms phase error. The low sidelobes of the thinned array are advantageous in the context of an air traffic control radar system as described below because the individual beams which are generated tend to reject returns from adjacent beams. Antenna beam 610 produced by array antenna 18b has the same general appearance in the azimuth plane as in the elevation plane, and may be considered to be a "pencil" beam as opposed to a fan beam.

Array antenna 18b of FIGURE 1 could be designed to provide a fan beam corresponding to that of the ASR-9 mechanically scanned system. However, such a fan beam has the disadvantage that the transmitted power is distributed over a larger volume than a pencil beam, and the power density is therefore lower than that of a pencil beam, so detection of distant targets requires greater power from each TR module; put another way, the use of a fan beam reduces the detectable target range for a given maximum TR module output power. Furthermore, generation of a fan beam requires a considerable amount of amplitude and phase tapering of the aperture distribution, which as mentioned above reduces overall power gain, and also reduces efficiency.

According to an aspect of the invention, active array antenna 18b of FIGURES 1 and 2 is capable of producing pencil beams in certain discrete azimuth and elevation directions. The shape of the beams is determined, in part, by the relative phase shifts imparted to the RF pulses transmitted by each antenna element, and the phase shifts are controlled by phase shifters associated with each TR module. The phase shifts required for a pencil beam in a given direction are well known. FIGURE 6a illustrates as ellipsoids each of the beams produced in one octant (one-eighth of a hemisphere) in a volume scan mode of operation, while FIGURE 6b illustrates the beams produced in the same octant in a short-range mode of operation. Each antenna 18 in FIGURE 1 produces coverage in two octants, together corresponding to one quadrant (one-quarter of a circle or hemisphere). Thus, antenna 18b produces the beams illustrated in FIGURE 6a and a similar number of additional beams (the exact number is not the same because FIGURE 6a illustrates the on-axis beams which overlap the two octants). The azimuth angle, ordinarily designated ϕ , is indicated both in millicosines and in degrees relative to the projection $\phi = 0^\circ$ of broadside line 24 (FIGURE 1) into the horizontal x-y plane.

At the left of FIGURE 6a, line 616 represents the azimuth broadside direction, and line 618 near the bottom of the FIGURE represents 0° elevation. Line 620 at the right represents the 45° off-axis contour, and line 622 at the top represents 60° , the uppermost elevation angle of interest. As illustrated in FIGURE 6a, the antenna is capable of producing pencil beams at all elevation angles of interest, ranging from about 0° to about 60° . In the azimuth direction, the beams are generated from $\phi = 0^\circ$ to $\phi = 45^\circ$; another antenna array 18 on an adjoining face of structure 10 of FIGURE 1 continues the scan beyond the 45° illustrated in FIGURE 6a.

The elevation angle may be scanned up to 90° in elevation above the horizon in order to extend the surveillance coverage volume and eliminate the "cone of silence" above 60° in the current embodiment. The elevation angle may also be scanned down to 90° below the horizon (if tilt angle is appropriate) in order to accommodate siting peculiarities such as a mountain top, or cliff.

As illustrated in FIGURE 6a, the pencil beams are generated at 13 discrete elevation angles. In the azimuth direction, the number of pencil beams depends upon the elevation angle. At the lowest elevation angle (nominally 0°), 20 off-axis antenna beams 601b, 601c, ..., 601g, ..., 601u are provided in the illustrated octant. Another 20 off-axis antenna beams occur at the lowest elevation angle in the complementary octant (not illustrated), which, together with the on-axis pencil beam 601a, make a total of 41 discrete beam positions in azimuth. While beams 601 are nominally at zero degrees elevation, the beam centers are actually centered at an elevation angle of about 1.2° , so that the 3 dB beamwidth (about 3°) of each pencil beam nominally provides coverage down to ground level. Those skilled in the art realize that coverage down to ground level may cause ground clutter and result in unwanted returns, which may be dealt with by signal processing. Each beam 601 nominally overlaps the adjoining beam 601 at the 3dB contour. The actual beam overlap may differ from 3dB, as described below in conjunction with the discussion of gain margin.

At the next higher increment of elevation angle in FIGURE 6a, which is centered on 3.765° in elevation, a further set of 21 off-axis beams 602a, ..., 602u appear at various non-zero azimuth angles in the octant illustrated in FIGURE 6a. Beams 602 are shifted in azimuth relative to beams 601, and as a result there is no on-axis beam 602. For example, the centers 661a, 661b and 662a of beams 601a, 601b and 602a, respectively, form a triangle illustrated by dash-lines 698, as illustrated in more detail in FIGURE 6b; the cumulation of such mutually staggered beams results in a triangular lattice. Each beam 601a, 601b and 602a nominally overlaps the adjacent beams at the 3dB contour. It should be emphasized that this overlap is only conceptual, as the beams are generated sequentially and not simultaneously. There are a total of $2 \times 21 = 42$ beams 602 in a quadrant.

At the next higher increment of elevation angle in FIGURE 6a, which is 8.043° , a further set of one on-axis beam 603a, and 20 off-axis beams 603b, ..., 603u result in a total of 41 beams in a quadrant. A total of twenty off-axis beams are illustrated in FIGURE 6a as beams 604a-604t, all of which are centered on 12.381° in elevation (40 beams/quadrant). Similarly, as illustrated in FIGURE 6a, 19 off-axis beams 605b, ..., 605t, and an on-axis beam 605a are all centered on an elevation angle of 15.829° (39 beams/quadrant). Table I tabulates row

EP 0 509 843 A2

numbers from 1 to 13, the corresponding elevation angles, number (#) of pencil beams illustrated in FIGURE 6a, and beam designations for the octant of the arrangement of FIGURE 6a. The total number of beams (Total #) in a quadrant is also given.

5

TABLE I

	<u>Row</u>	<u>Angle</u>	<u>#</u>	<u>Beam Designation</u>	<u>Total#</u>
	1	1.200°	21	601a...601u	41
10	2	3.765	21	602a...602u	42
	3	8.043	21	603a...603u	41
	4	12.381	20	604a...604t	40
15	5	15.829	20	605a...605t	39
	6	19.627	20	606a...606t	40
	7	24.037	20	607a...607t	39
	8	28.806	18	608a...608r	36
20	9	34.006	18	609a...609r	35
	10	39.527	16	610a...610p	32
	11	45.273	15	611a...611o	29
25	12	51.153	13	612a...612m	26
	13	57.235	12	613a...613l	23

30 As may be discerned by reference to Table I, the number of beams tends to decrease with increasing elevation angle. This result is to be expected, as the volume of space to be covered decreases with increasing elevation angle.

Each of the beams of FIGURE 6a overlaps its neighbors sufficiently to provide continuous coverage of the volume from nominally zero elevation to an elevation angle of about 60°, and $\pm 45^\circ$ in azimuth from 0°. As mentioned, the pencil beams nominally overlap at their 3 dB power points, so that the two-way (transmit and receive) loss is 6 dB. Four arrays of beams such as that of FIGURE 6a, resulting from an arrangement such as that illustrated in FIGURE 1, can provide 360° coverage in azimuth, and up to 60° in elevation, which is sufficient for aircraft control. The sequential generation of the pencil beams is described in greater detail below. Regions 6100, 6110 and 6101 of FIGURE 6a are regions, described below in relation to one embodiment of the invention, in which the beams are provided with pulse durations of 100, 10 and 1 μ S, respectively, in the volume surveillance operating modes.

FIGURE 6c is similar to FIGURE 6a, and corresponding portions are designated by like reference numerals. While FIGURE 6a represents the beams used for the primary volume scan or surveillance, the beams of FIGURE 6c are used for a short-range surveillance and for other short-range operating modes such as final approach control. As a result of these different uses, the beams of FIGURE 6c represent beams which are required to provide response and accuracy at relatively short range, and therefore represent beams in which the transmitted pulse width or duration is much less than that used for volume surveillance. Thus, in one embodiment of the invention, the beams 601, 602 and 603 of FIGURE 6a represent beams with a pulse width of 100 μ S, while the short-range beams of FIGURE 6c result from transmissions with 1 μ S pulse widths.

50 In the octant of FIGURE 6c, 21 beams designated 614a through 614 μ may be generated at an elevation angle of 2.0°, a further 21 beams 615a-615 μ may be generated at an elevation angle of 7.205°, and 21 more beams 616a-616 μ may be generated at an elevation angle of 12.456°. There are 41 beams 614, 42 beams 615, and 41 beams 616. These three "layers" of beams are selected to be at different elevation angles than the beams of FIGURE 6a, so that the three "layers" of FIGURE 6c cover roughly the same total elevation angle as the lowermost four "layers" (beams 601, 602, 603 and 604) of FIGURE 6a. This is done in order to reduce the overall time spent in short-range scanning, and is possible because the gain margin (described below) is greater for the short-range operating mode, whereby each beam of the short-range operating mode can overlap the adjacent beam farther from the beam peak, for example at the 7.0 dB contour rather than at the 3.0 dB

EP 0 509 843 A2

contour.

FIGURE 7 is a view of the 13 beams which can be "visible" at any particular azimuth angle in the arrangement of FIGURE 6a, plotted as altitude in feet versus slant range in nautical miles. While the beam contours of FIGURE 8 generally exhibit increasing angular coverage as elevation increases, their altitude coverage depends upon the range at which a field strength measurement is made. Thus, in FIGURES 7, the width of the beams appears greater for those beams at lower elevation angles, because they are measured at a greater slant range than those at higher elevation angles. For surveillance use for airport terminal area aircraft control under current standards, the maximum range of interest is defined as 80 nautical miles, which corresponds to 110 km, and the maximum altitude of interest is 24,000 feet (7300 meters). For purposes of definiteness, the beams of FIGURE 7 are designated as though the representation were made at $\phi = 0^\circ$ (0° azimuth) of FIGURE 6a: the beam at the lowest elevation angle in FIGURE 7 is therefore 601a, the next 601b...and that at the highest elevation angle is 613a. The detection contour overlap of beams 601a and 602a (the confluence of their 3 dB contours) occurs at or beyond 60 nm, thereby guaranteeing that a target at 60 nm and below 24000 feet will be detected with the required probability and false alarm rates. That is, the target will be illuminated in sequence by both beams 601a and 602a, and at the target location the illumination by both beams assumes that targets in that direction will be detected by at least one of the beams with the required statistics. The probability contour antenna beam overlap guarantees that there is no reduction of margin for any target within the altitude and range specifications.

As so far described, the system according to the invention produces sequential pencil beams at various angles to cover the desired volume. There are a total of 463 beams in one quadrant. For coverage to 80 nm, a single pulse beam such as that of the ASR-9 must dwell for at least 744 μ S, and longer if the unambiguous range is to be extended. The product of 744 μ S times 463 is about 0.34 seconds. This is a satisfactory quadrant scan time. However, the ASR-9 uses Doppler filtering to eliminate returns from rain and ground clutter. Doppler filtering desirably requires a plurality of pulses per beam to produce good filtering and to eliminate range-Doppler blind zones. For example, the ASR-9 uses 18 pulses organized into two separate coherent processing intervals (CPI), of 8 pulses and 10 pulses each, at two different pulse repetition frequencies (PRF). This requirement raises the scan time to over six seconds for one 90° quadrant, without taking into account excess receive time which may be required for ambiguity reduction. Six seconds or more may be considered an excessive surveillance scan time.

According to an aspect of the invention, the overall scan time is reduced by making the pulse recurrence frequency (PRF) responsive to the elevation angle of the pencil beam currently being radiated. For example, referring to FIGURE 7, it can be seen that line 24000, representing a 24,000 foot ceiling, intersects beams 605a...613a at slant ranges which are less than 15 nm. From this, it can be seen that the dwell time which is required at high elevation angles is much less than 744 μ S, and the PRF can therefore be relatively increased for beams at higher elevation angles. This in turn reduces the dwell time for many of the beams, allowing the complete volume scan to be accomplished in less time than if the PRF were constant and based upon the maximum range. The PRF control aspect of the invention is described below in conjunction with FIGURES 10 AND 11, and is implemented as described below in conjunction with FIGURE 3b.

As mentioned, the long pulse width required to achieve the desired power for long-range operation results in a long minimum range, within which targets cannot be detected. According to another aspect of the invention, the transmitted pulse durations are changed in response to the elevation angle of the particular antenna beam being generated, with relatively short pulse widths being used at high elevation angles, where the slant ranges are short, and relatively long pulse durations being used for beams at low elevation angles, at which ranges are longer. While continuous variation could be used, it appears that operation in three discrete ranges of pulse-width produces acceptable results and may be simpler to implement. In a surveillance mode of a particular embodiment of the invention, 100 μ S pulses are used for beams at elevation angles corresponding to beam sets 601, 602 and 603 (region 6100) of FIGURE 6a, 10 μ S pulses are used for beam 604 (region 6101), and 1 μ S pulses are used for beams 605...613 (region 6101).

FIGURE 8a illustrates the beams of FIGURE 6a at a particular azimuth angle such as $\phi = 0^\circ$, plotted as elevation angle versus slant range. In FIGURE 8a, the ranges within which targets can be detected, using 100 μ S pulses for beams 601, 602 and 603, 10 μ S pulses for beams 604, and 1 μ S pulses for beams 605-613 of FIGURE 6a, is illustrated by shaded region or volume 810. Shaded region 810 is bounded on one side by line 24000, which is the 24,000 foot altitude contour. The 24,000-foot contour is curved because of the nature of the ordinate and abscissa. Shaded region 810 is bounded on the other side by lines 15, 801 and 150, representing ranges of 15 km, 1.5 km, and 150 meters, respectively. Note that up to about 10° elevation, targets cannot be detected within a volume designated 894, having a range extending to about 8 nm (15km), and from zero elevation to about 8° elevation angle, due to the relatively long 100 μ S pulse associated with beams 601a, 602a and 603a. Also, from about 8° elevation to about 16° , the minimum range is about one nautical mile due to the 10 μ S pulse

BEST AVAILABLE COPY

EP 0 509 843 A2

associated with beam 604a. Above an elevation angle of 16°, the 1 μS pulse allows target detection as close as about 150 meters. For aircraft control purposes, 150 meter detection is deemed to be adequately close.

According to a further aspect of the invention, the three additional lower beam sets 614, 615 and 616 illustrated in FIGURE 6c are periodically operated with short transmitter pulses, such as 1 μS, in order to provide close-in as well as long-range target detection. It should be noted that the strategy of using short pulses at higher elevation angles in the surveillance or volume scan mode eliminates the need for a second dwell at high elevation angles for short-range target detection, which further aids in reducing the overall volumetric scan time.

FIGURE 8b is similar to FIGURE 8a, and corresponding portions are designated by like numerals. In FIGURE 8b, beams 614, 615 and 616 correspond to the beams of FIGURE 6c, and have their 7 dB contours overlapping at dash line 15, representing about 8nm or 15 km, the outer extreme of shaded volume 814. Shaded volume 814 represents the region within which targets are detected with high reliability in the approach mode, and extends from about 150 meters to 15 km, and to about 15° elevation.

Range ambiguity results when a pulse is transmitted, and the radar receives a return from a prior pulse beyond the range defined by the PRI. FIGURE 9 illustrates a time line, with equally spaced times T0, T1, T2,.... If targets in the range corresponding to T0 to T1 or T1 to T2 are of interest, and pulses are transmitted at times T1, T2, T3,...., a target at 1 1/2 times the desired range may reflect an earlier-transmitted pulse, which shows up as a range ambiguity. For example, a target at a range corresponding to time T0 - T1' in FIGURE 9 will reflect the pulse transmitted at time T0, which will return to the radar following the transmission of a pulse at time T1. If the returned signal is strong enough to be detected, it will be indistinguishable from a return generated by a target at the closer range T1 - T1'. Thus, the range of the target is ambiguous, as it may be T1-T1', or (T1-T1') plus multiples of (T0-T1). The strength of returns from targets decreases by a factor which is often expressed as being inversely proportional to the fourth power of range. In those instances in which propagation conditions are good and the radar transmitter and receiver exceed power and sensitivity specifications, respectively, large targets may produce discernible signal from well beyond the design range. This may be avoided by reducing the PRF, so that the PRI becomes longer than the range at which the most distant target of interest resides. In FIGURE 9, if the PRF is halved, as by transmitting only during even-numbered times T0, T2,...., the radar listening time is doubled, and the range from which undesired returns can be received is doubled. This is desirable in that the strength of undesired returns is reduced by a factor 2⁴ = 16, tending to reduce the likelihood of receiving an unwanted return. This strategy, however, has the effect of doubling the dwell on each beam, without increasing the useful data. The use of PRFs lower than necessary for the desired range, therefore, increases the time required for volumetric scan. Thus, a high PRF reduces the scan duration requirement, but introduces range ambiguity problems.

The use of a high PRF, as described above, can create anomalous or ambiguous results from targets at longer ranges than those intended to be detected. When Doppler filtering is used with a high PRF, an additional problem arises. To determine Doppler filter width (FW) in meters/sec, the equation

$$FW = \frac{V_{max}}{N} = \frac{\lambda PRF}{2N} \quad (1)$$

can be used, where:

V_{max} is the unambiguous velocity interval;
N is the number of pulses per set;
λ is wavelength in air; and
PRF is pulse recurrence frequency in hertz.

As can be seen from Equation (1), the Doppler Filter width is directly proportional to the PRF. At a λ of 0.107 meters (corresponding to about 2.8 GHz), with a PRF of 5 KHZ the unambiguous velocity interval is 267.5 meters per second, and N=8 pulses in each Doppler dwell yields a Doppler filter width of

FW = 0.107 (5000)/16 = 33.4 meters/sec which corresponds with 85 knots. A Doppler filter width as large as 65 knots is disadvantageous because most targets moving approximately tangentially relative to the radar will fall into the lowest Frequency Doppler filter, and will be obscured by other such targets or by clutter, and changes in PRF will have to be very large to move the targets out of the clutter filters. The use of Doppler filters thus seems to require low PRFs. This would seem to make it undesirable to use high PRFs for any of the beams.

According to another aspect of the invention, a beam scan pulsing regimen is used which for simplicity is termed "beam multiplex" (BmPX) which has the benefit of low scan duration requirement while reducing range ambiguity. In BMPX operation, the radar cycles through a subset of beam positions, which may be a number such as eight, pulsing each beam of the subset once during each transmit/receive interval before moving on to the next beam of the subset, with the transmitter (the source of transmitter pulses) operating at a high PRF but each of the beams operating at a lower PRF as a result of the sequencing. The data representing returns from targets are stored for data processing. After the subset of beams has been so pulsed, the scanning (transmitting a pulse during each transmit/receive interval, waiting for returns, storing the returned data) begins again

EP 0 509 843 A2

at the first beam of the subset and continues through all beams of the set. This continues until a sufficient number of pulses have been transmitted from each beam of the subset to provide proper inputs to the Doppler filters. Thus, each beam operates at a low PRF, and the set of pulse returns for that beam has a low effective PRF, so that the signals can be filtered in digital signal processing block 68 of FIGURE 3 by narrow-band Doppler filters (described below in conjunction with FIGURES 13-16) for good range rate separation. Notwithstanding the low effective PRF of each beam, the volumetric scan rate is high because the number of active beams is high. Thus, in beam multiplex operation, that is to say that all the beams of the subset are time-division multiplexed or interleaved from pulse recurrence interval (PRI) to PRI.

In general, the transmitter power, gain margin, beam overlap, antenna aperture and beamwidth, off-broadside antenna gain reduction, atmospheric loss as a function of elevation angle, and the like, are selected or balanced so that the same number of pulses must be transmitted on each beam and processed by the signal processor at $\phi = 0$, regardless of elevation angle. As further described below, this base number of pulses is 18 in one embodiment of the invention, broken into groups of 8 pulses at a first PRF and an additional 10 pulses at a second PRF.

The loss of margin or reduction of power gain attributable to scanning of beams to an off-broadside direction could be compensated for by increasing the transmitter power and/or antenna aperture. The solidstate RF amplifiers are already operating at full power, so transmitter power cannot be increased without the use of variable attenuators to reduce the power at broadside, so that it may be relatively increased off-broadside, and changing antenna aperture is extremely costly. Instead, according to a further aspect of the invention, the loss of margin or reduction of power gain which occurs when scanning the phased-array pencil beams in azimuth far from the on-axis condition is ameliorated by adaptively integrating (transmitting, receiving and processing) a relatively larger number of pulses than in the on-axis condition, as described in more detail below. The larger number of pulses undesirably increases the volumetric scan time, but is considered a desirable tradeoff in view of the cost of alternatives such as increasing the antenna aperture, the transmitted power, or both. The adaptive pulse integration approach is made viable because of the volumetric scan time decrease (time occupancy saving) attributable to beam multiplex technique, PRF and pulse duration variation with elevation angle.

FIGURE 10 summarizes the time occupancy for one system, such as that of FIGURE 3, according to an embodiment of the invention, operated in both surveillance and short-range modes. A triangular lattice of elements on an antenna array tilted 15° in elevation θ , as in FIGURE 1 is assumed, with the beam structure assumed to be that of FIGURE 6. A 1dB system margin is assumed. The measurement of margin in this embodiment is made at azimuth angle $\phi = 0$, and at an elevation angle of 1.2° (above the horizon), corresponding to 13.8° below broadside of the array. For this purpose, margin means excess power gain over that required to meet the specified probability of detection.

In FIGURE 10, the numeral "1" in row 1 of Column I, under the designation "Scan #" represents scanning of all 41 pencil beams 601 of FIGURE 6 (hence, it represents scanning of a quadrant). Column II, "el(deg)", lists the elevation angle at which the center of the pencil beams occur, which is 1.200° for scan # 1. Column III, "rng(km)", specifies the slant range in kilometers corresponding to 24000 feet or, in the case of the 1.2° beam, the instrumented range, and hence represents the range within which targets of interest lie. For scan # 1, the range is 111.12 km, corresponding to 60 nm. Column IV "pw(μ sec)" lists the corresponding transmitter pulse width in microseconds for the volume scan mode of operation. Columns V and VI, "prf1(hz)" and "prf2(hz)", are the PRFs of successive sets of N pulses on each beam. The higher PRF, namely prf2, is selected to provide the desired slant range at the particular elevation angle of the scan. A second PRF (PRF 1) is provided to reduce the effects of blind ranges in relation to the Doppler filters. PRF1 is selected to be $4/5$ of PRF 2, to adequately shift returns from one Doppler Filter to the next. The "duty (%)" of column VII tabulates the duty cycle calculated from pulse width and the higher PRF. For example, for Scan #1 the duty cycle is calculated as $1340 \times 100 \times 10^{-6} \times 100 = 13.4\%$. The duty cycle may be relevant in establishing the peak and average output power of a TR module. Column VIII, "time (msec)", lists the total time in milliseconds required for scanning $\pm 45^\circ$ (one quadrant) in azimuth at each elevation, with two sets of pulses (one set at PRF1, the other set at PRF2) for each pencil beam at that elevation. The "pulses" of column IX lists the total number of transmitter pulses for the scan at one elevation in one quadrant.

While the time tabulated in column VIII of FIGURE 10 is given in terms of the time for scan at each elevation, there is no necessity that all scans at one elevation be completed before moving on to the next elevation, and in principle the individual beams can be scanned in any order. Thus, scan 1 of FIGURE 10 operates with 100 μ S pulses, and addresses each of the 41 beams of the lowest elevation angle (21 beams 601 of FIGURE 6 in one octant and 20 corresponding beams in the associated octant) with at least eight pulses at a PRF of 944 Hz, and then with at least ten further pulses at a PRF of 1180 Hz for the beam at azimuth broadside. The duration of a cycle at a PRF of 944 Hz is about 1.06 msec, and at 1180 Hz is about 0.848 msec, so 18 pulses per beam consumes about $(8 \times 1.06) + (10 \times .848) = 16.95$ msec. The time for a full azimuth quadrant ($\phi = \pm 45^\circ$) scan at

**This Page is Inserted by IFW Indexing and Scanning
Operations and is not part of the Official Record**

BEST AVAILABLE IMAGES

Defective images within this document are accurate representations of the original documents submitted by the applicant.

Defects in the images include but are not limited to the items checked:

- ☐ BLACK BORDERS
- ☐ IMAGE CUT OFF AT TOP, BOTTOM OR SIDES
- ☐ FADED TEXT OR DRAWING
- ☐ BLURRED OR ILLEGIBLE TEXT OR DRAWING
- ☐ SKEWED/SLANTED IMAGES
- ☐ COLOR OR BLACK AND WHITE PHOTOGRAPHS
- ☐ GRAY SCALE DOCUMENTS
- ☐ LINES OR MARKS ON ORIGINAL DOCUMENT
- ☒ REFERENCE(S) OR EXHIBIT(S) SUBMITTED ARE POOR QUALITY
- ☐ OTHER: _____

IMAGES ARE BEST AVAILABLE COPY.

As rescanning these documents will not correct the image problems checked, please do not report these problems to the IFW Image Problem Mailbox.